Available online at www.sciencedirect.com
ScienceDirect
Journal of Controlled Release 128 (2008) 41–49
journal of controlled release
www.elsevier.com/locate/jconrel

Dexamethasone acetate encapsulation into Trojan particles

Carolina Gómez-Gaete [a,b,c], Elias Fattal [a,b], Lídia Silva [a,b], Madeleine Besnard [a,b], Nicolas Tsapis [a,b,*]

[a] Univ Paris Sud, UMR CNRS 8612, Faculté de Pharmacie, Châtenay-Malabry, France
[b] CNRS, UMR 8612, Faculté de Pharmacie, Châtenay-Malabry, France
[c] Facultad de Farmacia, Universidad de Concepción, Concepción, Chile

Received 15 January 2008; accepted 15 February 2008
Available online 4 March 2008

Abstract

We have combined the therapeutic potential of nanoparticles systems with the ease of manipulation of microparticles by developing a hybrid vector named Trojan particles. We aim to use this new delivery vehicle for intravitreal administration of dexamethasone. Initialy, dexamethasone acetate (DXA) encapsulation into biodegradable poly(D,L-lactide-co-glycolide) (PLGA) nanoparticles was optimized. Then, Trojan particles were formulated by spray drying 1,2-Dipalmitoyl-*sn*-Glycero-3-Phosphocholine (DPPC), hyaluronic acid (HA) and different concentrations of nanoparticle suspensions. The effect of nanoparticles concentration on Trojan particle physical characteristics was investigated as well as the effect of the spray drying process on nanoparticles size. Finally, DXA *in vitro* release from nanoparticles and Trojan particles was evaluated under sink condition. SEM and confocal microscopy show that most of Trojan particles are spherical, hollow and possess an irregular surface due to the presence of nanoparticles. Neither Trojan particle tap density nor size distribution are significantly modified as a function of nanoparticles concentration. The mean nanoparticles size increase significantly after spray drying. Finally, the *in vitro* release of DXA shows that the excipient matrix provides protection to encapsulated nanoparticles by slowing drug release.

Keywords: Trojan particles; Nanoparticles; Dexamethasone; Crystalline drug; Spray drying

1. Introduction

Spray drying is a single step continuous process commonly used in the pharmaceutical and food industry to produce dry particles by atomization of a liquid (solution, suspension, emulsion, etc). For pharmaceutical applications, spray drying allows to obtain relatively monodisperse microparticles with a high percentage of encapsulation. Microparticles have the important advantage to avoid fast clearance after intraocular administration increasing drug residence time [1,2]. However, due to their large size, microparticles are not able to diffuse within tissues. Although they do not induce long term release, nanoparticles can easily diffuse into a particular tissue and even penetrate within cells located in these tissues [3]. Unfortunately, nanoparticles are often difficult to manipulate as compared with microparticles. In their dry form, they have the tendency to aggregate and can be unstable in aqueous suspension due to hydrolysis and/or sedimentation [4].

Under those circumstances, a hybrid system, combining the advantages of nanoparticles from the therapeutic point of view with the facility of manipulation of microparticles, would be an interesting delivery vehicle for active molecules. A system with these characteristics using however non biodegradable polymers was first proposed by Tsapis et al. [5]. It was first shown that the choice of excipients used to formulate these hybrids systems, could either improve their physical properties or the stability of nanoparticles, and even allow to tune precisely nanoparticles release from the vehicle [6].

The development by spray drying of such a hybrid system for the administration of corticoids in the treatment of posterior segment eye diseases represents an interesting therapeutic

* Corresponding author. Univ Paris Sud, UMR CNRS 8612, Faculté de Pharmacie, 5 Rue Jean-Baptiste Clément, 92296 Châtenay-Malabry, France. Fax: +33 146619334.
E-mail addresses: nicolas.tsapis@u-psud.fr, ntsapis@gmail.com (N. Tsapis).

0168-3659/$ - see front matter © 2008 Elsevier B.V. All rights reserved.
doi:10.1016/j.jconrel.2008.02.008

opportunity. Considering that the administration by the systemic route of large quantities of corticoids can induce undesirable side effects and, that topical administration does not allow sufficient drug passage to the posterior segment, a therapy allowing direct release of drugs into the vitreous is often required for the effective treatment of posterior segment diseases [7,8].

Dexamethasone has demonstrated to be an efficient anti-inflammatory drug in the treatment of acute and chronic posterior segment eye diseases such as uveitis or affections that involve neovascularization, such as proliferative vitreoretinopathy or subretinal neovascularization [9–11]. Current treatments using corticoids are performed by direct injections of corticoid solutions or suspensions. However, direct injections of corticoids into the vitreous often require large boluses and repeated injections to ensure therapeutic levels over an extended period of time, leading to a reduction of patient compliance, or to an increased likelihood of complications [12]. Implants, developed to avoid the repeated injections, offer an good alternative [13,14]. Nevertheless, their principal disadvantage is that, sometimes, a large surgical incision is required [15]. Therefore, the incorporation of drugs within microparticles to be injected through fine needles into the vitreous represents a therapeutic opportunity to enhance drug retention in this cavity [16]. Microparticles encapsulating corticoids elaborated by spray drying has been widely developed for several routes of administration except for the intravitreal route [17–24]. Nevertheless, a hybrid system encapsulating corticoid-loaded nanoparticles has yet to be developed.

This article describes the development of a hybrid system named Trojan particles to deliver dexamethasone-loaded nanoparticles in the vitreous. Excipients such as 1,2-dipalmitoyl-*sn*-glycero-3-phosphatidylcholine (DPPC) and hyaluronic acid (HA) have been chosen to form Trojan particle matrix due to their biocompatibility and biodegradability. Although DPPC is biocompatible and biodegradable, only a few ocular formulations have used it [25,26]. Previous studies have demonstrated that a concentration of 33 mM of phospholipids is not toxic by intravitreal injection [27]. HA, a glycosaminoglycan naturally present in the vitreous, is widely used for pharmaceutical application [28–30] and has been shown to slow down drug release [31,32]. Dexamethasone acetate (DXA) encapsulation into poly(D,L-lactide-co-glycolide) nanoparticles was first optimized before Trojan particle formulation. The effect of nanoparticle concentration on Trojan particle physical characteristics was investigated. Finally, a comparison between the *in vitro* release of DXA from Trojan particles and free nanoparticles was performed under sink conditions.

2. Materials and methods

2.1. Materials

Poly (D,L-lactide-co-glycolide) (PLGA 75:25) Resomer RG756 was purchased from Boehringer-Ingelheim (Germany). Poly (vinyl-alcohol) (PVA) (87–89% hydrolyzed, MW 30,000–70,000), *N*-(2-hydroxyethyl) piperazine-*N*′-(2-ethanesulfonic acid) (HEPES), sodium chloride (NaCl) and Nile Red, were obtained from Sigma-Aldrich (France). Dexamethasone acetate (DXA) was provided by Chemos GmbH (Germany). 1,2-Dipalmitoyl-*sn*-Glycero-3-Phosphocholine (DPPC) was obtained from Genzyme (Switzerland) and hyaluronic acid, sodium salt 95% (HA) (MW = 1 000 k/Da) by Acros organic (France). The Fluorescent lipid CF-PE (1,2-Dioleoyl-*sn*-Glycero-3-Phosphoethanolamine-*N*-(Carboxyfluorescein)) was purchased from Avanti Polar Lipids (USA). Acetone, dichloromethane, absolute ethanol in analytical grade and acetonitrile in high-performance liquid chromatography (HPLC) grade were all obtained from Carlo Erba Reagents (France). Water was purified using a RIOS system from Millipore (France).

2.2. Nanoparticle preparation and characterization

2.2.1. Nanoparticle preparation

PLGA nanoparticles loaded with DXA were prepared by a solvent emulsion–evaporation technique. Briefly, 100 mg of PLGA was dissolved into 2.5 mL of dichloromethane and DXA was dissolved into 2.5 mL of acetone. Then, both organics solutions were mixed and pre-emulsified with 20 mL of a PVA aqueous solution (0.25% w/v) by vortexing at 3,200 rpm for 1 min (Mini Vortexer VWR, USA). The pre-emulsion was kept on ice and sonicated at 300 W for another minute using a Vibra cell sonicator (Bioblock Scientific, France). The organic phase was then evaporated at room temperature under gentle agitation (700 rpm). Nanoparticle suspension was then completed to 20 mL by weight. Amber vials were used throughout the process to provide protection against degradation by UV of DXA [33]. Non-encapsulated DXA crystals were visualized by optical microscopy (Leitz Diaplan microscope equipped with a Coolsnap ES camera (Roper Scientific, France). Crystals were eliminated by successive filtration of the nanoparticles suspension using Polyvinylidine difluoride (PVDF) filters (3.0, 1.2 and 0.45 μm consecutively).

2.2.2. Particle size and Zeta potential

Particle size and polydispersity index were determined using a Malvern Zetasizer Nano ZS (Malvern Instrument, UK) based on quasi-elastic light scattering. Size measurements were performed in triplicate following a 1/100 v/v dilution of the nanoparticle suspension in purified water at 25 °C. The polydispersity index range was comprised between 0 and 1. Zeta potential was measured using the same instrument at 25 °C following a 1/50 v/v dilution in a 1 mM NaCl solution.

To assess the influence of the spray drying process on nanoparticle size, Trojan particles elaborated only with DPPC as an excipient and 17% nanoparticles were dissolved in the same solvent used for spray drying and the size of suspended objects was measured using a Malvern Zetasizer Nano ZS (Malvern Instrument, UK). More precisely, 5 mg of Trojan particles were suspended into 7 mL of ethanol and vortexed for 30 s before adding 3 mL of water and vortexing. Size measurements were performed in the ethanol/water mixture (70:30 v:v, viscosity 2.4 cP and refractive index 1.364 at 20 °C). Controls were performed using microparticles containing only DPPC and nanoparticle suspension.

2.2.3. Encapsulation efficacy within nanoparticles

After crystal elimination by filtration as described previously, 2 g of nanoparticles suspension was ultracentrifuged (110,000 *g* for 30 min at 25 °C, ultracentrifuge Optima™ LE-80 K, rotor type 70.1, Beckman) to separate the soluble DXA in the supernatant from the nanoparticles. The temperature was kept at 25 °C to prevent recrystallization [34]. Nanoparticles were then dissolved into 2 mL acetonitrile, vortexed for 1 min and centrifuged at 9030 *g* for 5 min (Mini Spin Eppendorf centrifuge) to eliminate PVA that is not soluble in acetonitrile. Supernatants were filtered prior to analysis with a 0.45 μm PVDF filter. The quantity of DXA in the particles was determined by injecting 20 μL of the filtered solution in a Waters™ liquid chromatograph (HPLC) equipped with a Waters™ 600 pump, a Waters™ 7956 interface, a Waters™ 2996 photodiode array detector, a Waters™ 717 autosampler and a Waters™ Empower Login software. The analysis was performed at 238 nm using an Interchrom™ Reverse Phase Nucleosil 5 C18 column (150 × 4.0 mm) with a mobile phase composed of 40% acetonitrile and 60% water at 1 mL/min. All the analysis was performed at room temperature and experiments were performed at least in triplicate. The method showed satisfactory linearity between 0.25 and 40 μg/mL. To compare encapsulation results with previous studies on dexamethasone base (DXM) [35], we have chosen to express the mass of encapsulated DXA as the equivalent DXM mass.

2.2.4. Solubilization and in vitro release kinetics of dexamethasone acetate

The kinetics of solubilization of DXA in HEPES buffer was performed under sink conditions: drug concentration in the medium was kept 5 times lower than the saturation solubility of DXA in HEPES buffer (18 ± 2 μg/mL). An accurately weighed amount of DXA was added to a volume of 10 mM HEPES buffer saline (150 mM NaCl, pH 7.4), to reach a maximum concentration of about 3–4 μg/mL. Samples were protected from light and kept at 37 °C under stirring (150 rpm). At predetermined time intervals, an aliquot of the solution was analyzed by HPLC as described above after filtration through a 0.45 μm PVDF filter to eliminate unsolubilized DXA.

In vitro release of DXA from nanoparticles was carried out under sink conditions. After crystal filtration, 0.8 g of nanoparticle suspension were ultracentrifuged at 27,500 *g* for 20 min at 25 °C using the same ultracentrifuge described above. The centrifugation was carried out at lower speed to allow resuspension of nanoparticles without any modification of their size as checked by light scattering. After removal of the supernatant, nanoparticles were resuspended into 10 mL of 10 mM HEPES buffer saline (150 mM NaCl, pH 7.4) by vortexing. A vial was prepared for each time point, protected from light and kept at 37 °C under tangential stirring (150 rpm) (Heidolph-Titramax 1000, Germany). At predetermined time intervals, 2 mL of release medium were removed and ultracentrifuged at 110,000 *g* for 30 min at 25 °C and the supernatant was collected. All centrifuged supernatants were filtered on a 0.45 μm PVDF filter and stored at 4 °C until analysis by HPLC. Experiments were performed in triplicate.

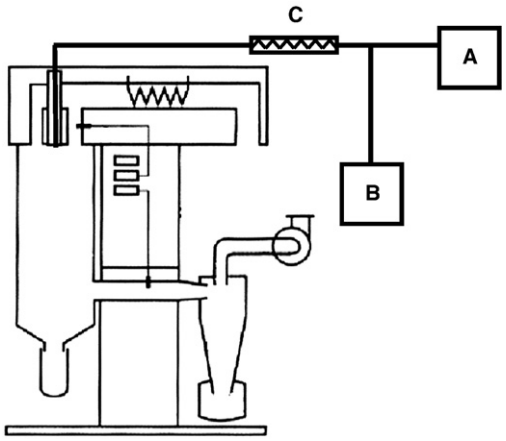

Fig. 1. Schematic representation of the spray drying device (mini spray dryer BÜCHI B-191) adapted with two gear pumps (A and B) and with an acetal helix (C) for in-line mixing of nanoparticles suspension and excipient solution.

2.3. Preparation of Trojan particles and yield calculation

Trojan particles were produced by spray drying. One or several batches of nanoparticles suspensions were used (0.1–0.5 g). After crystal elimination by filtration as described above, the nanoparticle suspension was ultracentrifuged (110,000 *g* for 30 min at 25 °C) to separate nanoparticles from soluble DXA in the supernatant. After removal of the supernatant, nanoparticles were resuspended into 25 mL of water just before being spray dried and maintained under moderate stirring, while fed into the spray-dryer. Additionally, Trojan particles were constituted of biodegradable and biocompatible excipients. An aqueous solution of HA was prepared dissolving 0.2 g of HA into 125 mL of ultra-pure water, under stirring at room temperature. An ethanolic solution of DPPC was prepared by dissolving 0.8 g of DPPC into 350 mL of ethanol absolute. Both aqueous and ethanolic solutions were mixed prior to spray drying.

Nanoparticle suspension and excipients solution were fed to the spray dryer (mini spray dryer BÜCHI B-191 (Flawil, Switzerland) using two digital gear pumps (Cole-Parmer Instrument Company) connected to an acetal helix (Fig. 1). Nanoparticle suspension was pumped at 1 mL/min and excipients were pumped at 16 mL/min. The helix provided efficient mixing of the solutions and the resulting flow was atomized through a 0.7 mm diameter two-fluid nozzle (co-current mode). Since ethanol is a very good solvent for DXA, this set-up was used to reduce as much as possible the contact time between nanoparticles and ethanol and consequently DXA leak from nanoparticles suspended in ethanol before spray drying. Spray drying conditions were the following: inlet temperature 110 °C; outlet temperature 53–55 °C; aspiration 100% and air flow air 600 l/h. The total amount of solids used was 2.2–3.0 g/L. The glass chambers of the spray dryer were protected from light. Powders were gathered from the collector vessel and stored at room temperature under vacuum in a dessicator immediately after spray drying to limit moisture uptake by samples between production and testing. The yield was calculated as a percentage by dividing the mass of the powder collected by the initial mass of solids in the solution prior to spray drying.

2.3.1. Trojan particle size distribution

The volume median geometric diameter (D_{50}) of the powders was measured by light diffraction using a Mastersizer 2000 equipped with a Scirocco dry disperser (Malvern Instruments, France) at a dispersing pressure of 1 bar. The refractive index used was 1.5. Each sample was measured in triplicate. Data obtained were expressed in terms of the particle diameter at 10%, 50% and 90% of the volume distribution (D_{10}, D_{50} and D_{90} respectively) and as the volume mean particle size (D[4.3]).

2.3.2. Scanning electron microscopy

Scanning electron microscopy (SEM) was performed using a LEO1530 microscope (LEO Electron Microscopy Inc, Thornwood, NY) operating between 1 and 3 kV with a filament current of about 0.5 mA. Powder samples were deposited on a carbon conductive double-sided tape (Euromedex, France). They were coated with a palladium-platinum layer of about 4 nm, using a Cressington sputter-coater 208HR with a rotary planetary-tilt stage, equipped with a MTM-20 thickness controller.

2.3.3. Tap density

Powder tap density (ρ) was determined using a tapping apparatus (Pharma test PT-TD1). Accurately weighed powder samples were filled into a 10 mL graduated cylinder and the height measured following 1000 taps which allowed the density to plateau. Assuming an efficient packing, the tap density of monodisperse spheres is approximately a 21% underestimate of the true particle density due to the void spaces between particles. Although polydispersity may reduce the void volume between particles, this is probably counterbalanced by an imperfect packing [36]. Measurements were performed in duplicate.

2.3.4. Confocal microscopy

Nile Red was added to organic solution prior to nanoparticles preparation in order to label exclusively the nanoparticles. Trojan particles were labelled adding 1% (w/w) fluorescent lipids (CF-PE) to the DPPC ethanolic solution before spray drying. Glass slides were examined with a Zeiss LSM-510 confocal scanning laser microscope equipped with a 1 mW helium neon laser and an Argon laser, using a Plan Apochromat 63× objective (NA 1.40, oil immersion). Red fluorescence was observed with a long-pass 560 nm emission filter under 543 nm laser illumination. Green fluorescence was observed with a 505–550 nm band-pass emission filter under 488 nm laser illumination. The pinhole diameter was set at 104 μm. Stacks of images were collected every 0.8 μm along the z axis.

2.3.5. Dexamethasone loading within Trojan particles

5 mg of the spray dried powder were weighed and dissolved first into 5 mL of ethanol before addition 5 mL of acetonitrile. After vortexing (2 min with each solvent), 1.5 mL of this solution was centrifuged (9030 g, 10 min) in order to eliminate the fraction of HA that was not soluble in both solvents. Then, the supernatant was filtered through a 0.45 μm polyvinylidine difluoride (PVDF) filter. The amount of DXA in the Trojan particles was determined by HPLC as described above.

2.3.6. In vitro release kinetics of dexamethasone

In vitro release of DXA from Trojan particles was carried out under sink conditions: drug concentration in the medium was kept at least 5 times lower than the solubility of DXA in HEPES buffer (18±2 μg/mL). 10 mg of Trojan particles were accurately weighed and suspended into 2.2 mL of 10 mM HEPES buffer saline (150 mM NaCl, pH 7.4) using a gentle vortex. A vial was prepared for each time point, protected from light and kept at 37 °C under tangential stirring (150 rpm) (Heidolph-Titramax 1000, Germany). At predetermined time intervals, 1.5 mL of release medium was removed, ultracentrifuged at 110,000 g for 30 min at 25 °C and the supernantant was collected. 700 μL of supernatant were mixed with 300 μL of acetonitrile and a centrifugation at 9030 g for 10 min (Mini Spin Eppendorf centrifuge) was performed to eliminate HA which was not soluble in acetonitrile. After filtration (0.45 μm PVDF filter), samples were stored at 4 °C until analysis by HPLC as described above. Experiments were performed in duplicate.

3. Results and discussion

3.1. Nanoparticles formulation

In a previous study, the encapsulation of dexamethasone base (DXM) into PLGA nanoparticles was optimized [35]. Optical microscopy observation of nanoparticle suspension revealed the presence of dexamethasone crystals, correlated with a low percentage of encapsulation. In addition, the release kinetics of DXM from nanoparticles was rather fast during the first hours. To improve drug encapsulation, a more hydrophobic form of the drug, DXA (partition coefficient: log P=2.91) was chosen to improve the affinity of the drug for the hydrophobic polymer matrix and reduce drug solubility in the external phase. Nanoparticles were elaborated by a solvent emulsion–evaporation method. A mixture of organic solvent (acetone and dichloromethane, 1:1) was used to ensure the correct solubilization of both DXA and the polymer. The main conditions such as surfactant concentration or sonication power were chosen according to our previous study [35]. Initially, a constant mass of DXA (10 mg) and polymer (100 mg) were fixed. Optical microscopy observations reveal the presence of DXA needle crystals of various sizes (Fig. 2). The presence of crystals means that a fraction of the active principle is not encapsulated, similarly to previous results obtained with DXM [35]. Crystallization is mainly due to the nature of the drug but is also favored by the organic solvent chosen for emulsification. Since acetone is a water miscible solvent, it can diffuse into the continuous phase, therefore increasing drug solubility. Then, as the organic solvent is evaporated, the drug solubility decreases and the free drug crystallizes. Similarly to DXM, DXA has a strong tendency to crystallize lowering its affinity for the polymer [35]. After elimination of crystals and the soluble DXA in the supernatant, the drug loading was quantified by HPLC. Only 0.6 mg of dexamethasone were encapsulated into 100 mg nanoparticles when starting initially with 10 mg DXA.

To evaluate the effect of initial DXA mass on drug loading, this parameter was varied between 2 and 25 mg. Independently of the

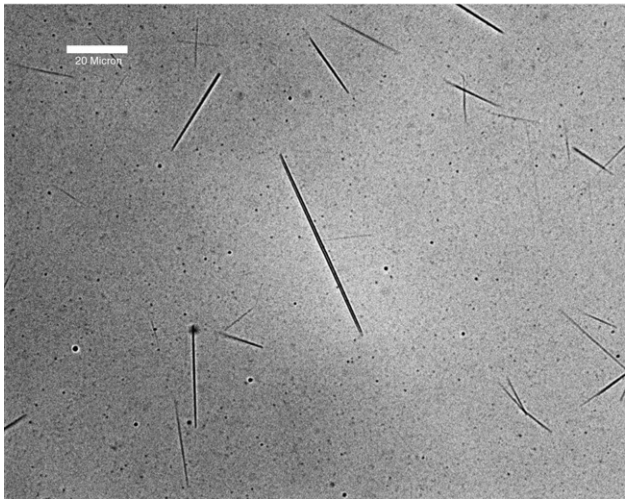

Fig. 2. Optical microscopy image of DXA crystals present in the nanoparticle suspension (scale bar=20 μm). Nanoparticles were prepared with 100 mg PLGA 75:25 and 5 mg DXA.

initial DXA mass, DXA crystals were observed. Drug loading increases when the initial mass of DXA increases, until it reaches about 1.3 mg DXM/100 mg nanoparticles for 5 mg DXA initial mass in the formulation (1.3 mg DXM=1.44 mg DXA). Drug loading then decreases and stabilizes around 0.6 mg DXM/100 mg nanoparticles (Fig. 3). These results suggest that there is a competition between molecular dispersion of the drug within the polymeric matrix and crystallization forces. Initially, DXA load increases until the matrix is saturated with the drug (initial DXA mass ≤ 5 mg). Then, as the number of crystals increases, crystallisation becomes the driving force and contributes to reduce the amount of drug encapsulated. Finally, an equilibrium is reached between crystallized and encapsulated DXA [35]. Although the trend in drug loading is very similar to what was observed with DXM, the optimal drug loading is about 6 fold higher using DXA. Since DXA has a greater affinity for the polymer matrix because of its hydrophobic nature, replacing DXM by DXA indeed improves drug loading within nanoparticles. Monodisperse nanoparticles were obtained independently of the amount of encapsulated drug, with a mean diameter (±width) around 220±54 nm and polydispersity indices below 0.1 (n=6). The zeta potential was negative −4.2±0.6 mV (n=3). These values do not differ from unloaded nanoparticles.

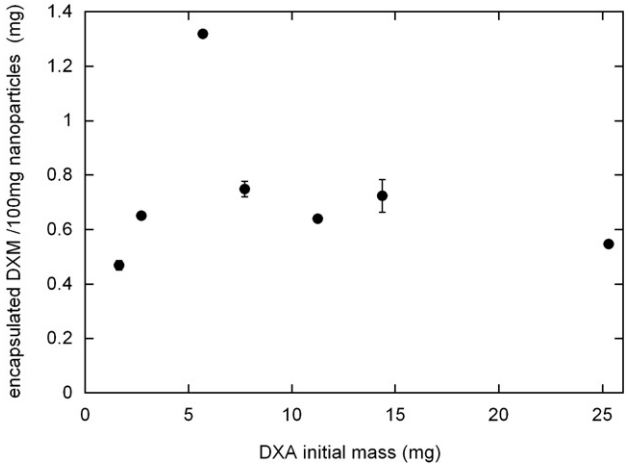

Fig. 3. Drug loading within nanoparticles as a function of the initial mass of DXA (mean±SD, n=4). Drug loading is expressed as dexamethasone base (DXM) to compare encapsulation results with our previous studies [35]. Nanoparticles were prepared with 100 mg PLGA 75:25.

An *in vitro* release study of the drug from loaded nanoparticles (1.3 mg DXM/100 mg nanoparticles) was performed under sink conditions (Fig. 4). The release profile shows a burst effect with about 90% of the loaded drug released during the first 4 h. This massive release can be related to the drug adsorbed onto nanoparticle surface. After the initial burst, a slower release is observed with the remaing 10% of the drug being released before 72 h. On the other hand, the DXA solubilization kinetics study in buffer HEPES under sink conditions, shows that all the DXA solubilizes in the release medium within 1.5 h. This control experiment demonstrates that DXA release from nanoparticles is controlled by the interaction of the drug with the polymer matrix and not by drug solubilization.

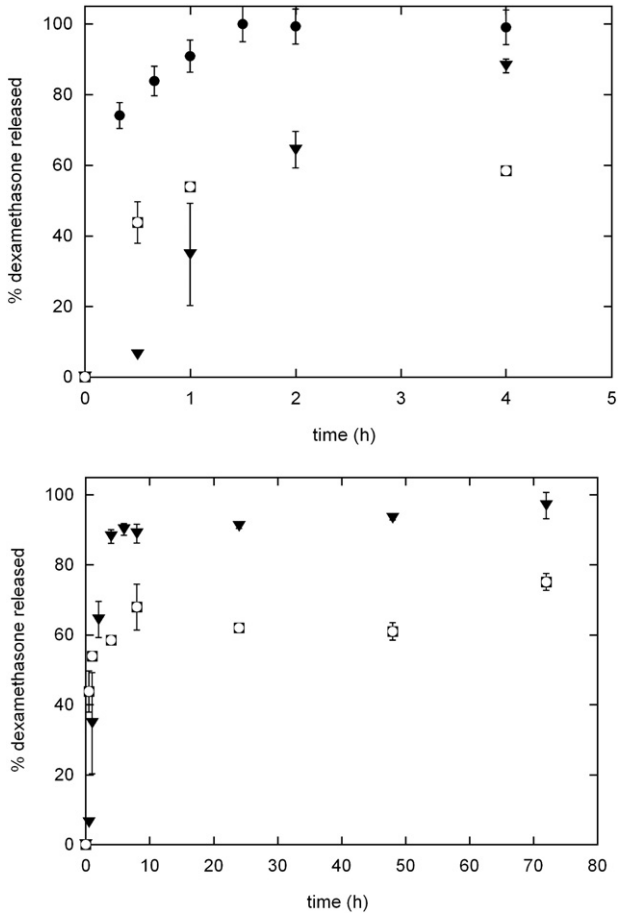

Fig. 4. Top: kinetics of solubilization of DXA drug in HEPES under *sink conditions* (●) and *in vitro* release profile of DXA from nanoparticles (▼) and from Trojan particles (◘) in HEPES buffer under *sink conditions*. Bottom: Longer times *in vitro* release profile of DXA from nanoparticles (▼) and from Trojan particles (◘) in HEPES buffer under *sink conditions*. Results are expressed as the percentage of the initial DXA load (mean±SD, n=3). Nanoparticules were formulated with 5 mg DXA and 100 mg PLGA. Trojan particles were formulated with 0.1 g nanoparticles, 0.8 g DPPC and 0.2 g HA in a total volume of 500 mL (350 mL ethanol/150 mL water).

3.2. Trojan particles formulation

DXA loaded nanoparticles were incorporated within previously optimized microparticles made of DPPC and HA. Indeed, a previous study has shown that DPPC microparticles are unstable and strongly aggregated (Gómez Gaete 2008, *accepted for publication in European Journal of Pharmaceutical Sciences*) and that the addition of HA to the formulation increases the stability of DPPC powders by preventing phospholipids rearrangement upon aging. Additionally, HA leads to an increase of particle size and a decrease of aggregation due to morphological change: pure DPPC particles are dense spheres whereas DPPC-HA microparticles are hollow shells (Gómez Gaete 2008, *accepted for publication in European Journal of Pharmaceutical Sciences*). The morphological change arises from a modification of the Peclet number of the solution before spray drying induced by the addition of HA. The Peclet number corresponds to the ratio of the mixing time of the chemicals in the droplet over the drying time of the droplet. Since HA is a large molecule (MW ~ 1000 kDa) it does not have the time to diffuse towards the center of the droplet as it dries. This later situation corresponds to a large Peclet number. Nanoparticles were suspended in a small volume of water just before being spray dried. Since ethanol is a very good solvent for DXA, it is likely that DXA would leak from nanoparticles suspended in ethanol before spray drying completion. Therefore, to reduce as much as possible the contact time between nanoparticles and ethanol, nanoparticles suspension was pumped to the spray dryer nozzle using a different pump than the one used for the ethanol/water mixture containing the excipients.

Fig. 5 (left), shows a SEM image of microparticles produced by spray drying DPPC and HA without nanoparticles. Microparticles are spherical with a smooth surface. Confocal microscopy has shown that most particles are hollow shells (Gómez Gaete 2008, *accepted for publication in European Journal of Pharmaceutical Sciences*). One of the particles in Fig. 5 is broken further revealing the morphology. Trojan particles are also rather spherical, but their surface is slightly irregular (Fig. 5, right). Close examination of Trojan particle surface indeed indicates that the roughness arises from the presence of nanoparticles (Fig. 5, bottom).

In order to check the influence of nanoparticles on the hollow morphology and to better observe the distribution of nanoparticles, confocal microscopy was performed after, labelling nanoparticles in red (Nile Red) and microparticle matrix in green (CF-PE). Confocal slices show that the vast majority of Trojan particles are hollow shells independently of nanoparticles concentration up to 33% (w/w). In addition, nanoparticles remain individualized and are homogeneously distributed within the shell (Fig. 6).

The influence of nanoparticles concentration on microparticle size distribution was evaluated (Table 1). As nanoparticle concentration increases, D_{10} is not modified. However, D_{50} decreases from 6.7 to 6.4 μm and D_{90} from 16.8 to 15.2 μm. A decrease is also observed for D [4.3] from 8.0 to 7.4 μm. A t-test reveals that these modifications are not significant ($p > 0.05$). These results are in agreement with Sham et al. [37] who have worked at low nanoparticle concentration and have found that the

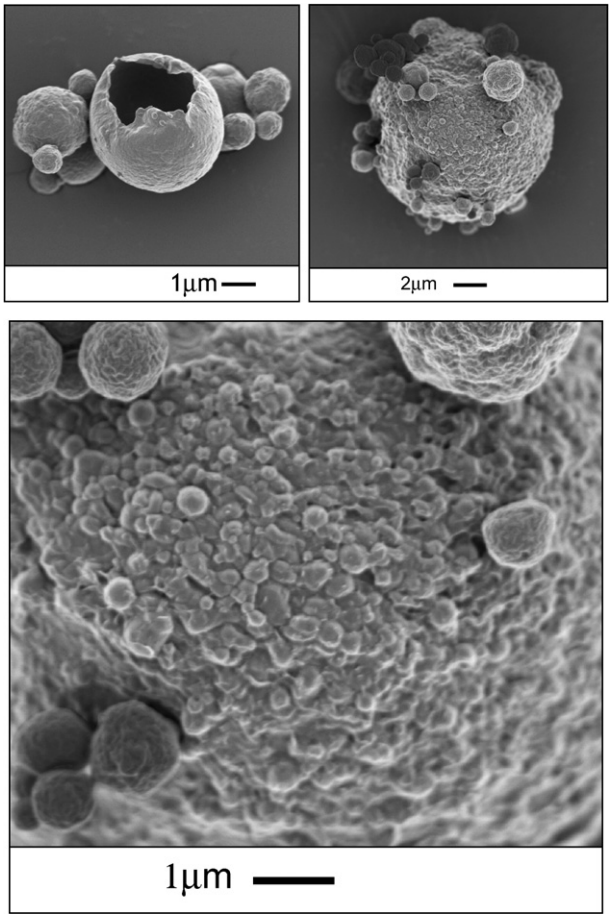

Fig. 5. SEM images of spray-dried powders. Top-left: Microparticles prepared with 0.8 g DPPC and 0.2 g HA in a total volume of 500 mL. Top-right: Trojan particles prepared with 0.8 g DPPC, 0.2 g HA and 0.1 g nanoparticles in a total volume of 500 mL. Bottom: Close-up on Trojan particle surface: one can distinguish nanoparticles.

size distribution of microparticles is independent of the presence of nanoparticles. Our results are partly in agreement with those of Hadinoto et al. [38] who have observed a significant reduction of microparticle size that is attributed to an increase of fine particles. In our case, however, D_{10} remains constant which proves that the fraction of fine particles is not modified. In contrast, Tsapis et al. [5] have observed that an increase of nanoparticles concentration leads to an increase in microparticle size, which was attributed to a pronounced effect of the Peclet number due to the high nanoparticle concentration used (up to 80%). In our system, the Peclet number is governed by HA concentration and therefore nanoparticle concentration do not play an important role (Gómez Gaete et al, accepted for publication in European Journal of Pharmaceutical Sciences).

There is no obvious effect of the concentration of nanoparticles on the yield of the process which remains around 36 ± 9%. Nanoparticle concentration does not seem to have an influence on powder tap density ($\rho = 0.073 \pm 0.002$ g/mL) as already observed by Hadinoto et al. [39] for polyacrylate nanoparticles. Since microparticles containing DPPC-HA are already hollow due to the presence of HA, the low concentrations of nanoparticles do not modify drastically the morphology and

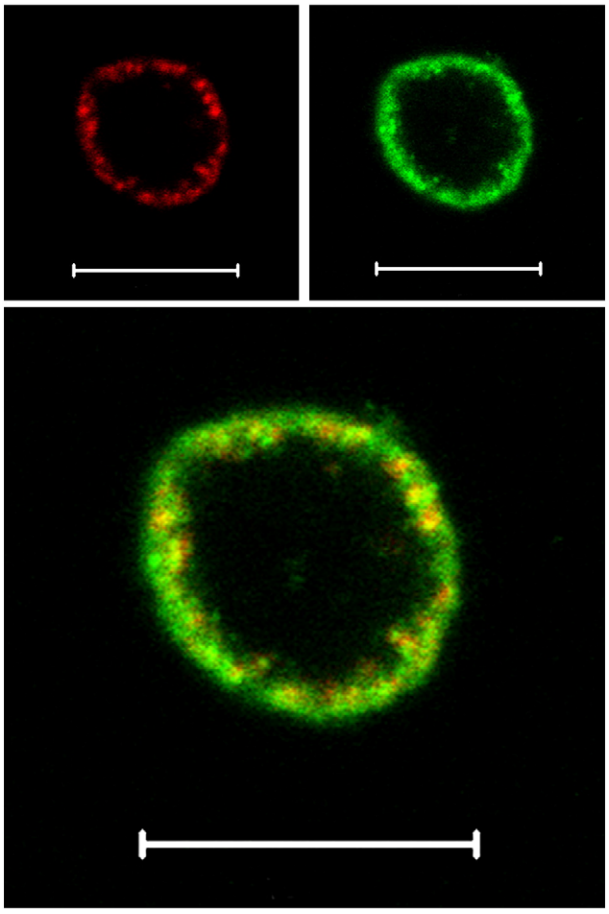

Fig. 6. Confocal microscopy image of a typical Trojan particle containing 9% (w/w) nanoparticles. Top-left: Red fluorescence corresponds to nanoparticles labelled with Nile Red. Top-right: Green fluorescence corresponds to lipid labelling with CF-PE Bottom: Superposition of both images. Scale bars represent 10 μm.

consequently the tap density. In contrast to results obtained by Tsapis et al. [5] where nanoparticle concentration governs the Peclet number of the system and therefore microparticle density, in our formulation HA concentration governs the Peclet number and therefore microparticle density.

3.3. Effect of spray drying on nanoparticle size

The mean nanoparticle size was measured before spray drying and after re-dissolving Trojan particles. The mean particle size increased from 200±60 nm to 230±100 nm. A *t*-test was performed to compare the size of nanoparticles before and after spray drying. Results indicate that they differ significantly ($p<0.05$). During the drying process, a solid shell forms when capillary attractions due to evaporation become stronger than repulsions between nanoparticles, then nanoparticles stick together due to Van der Waals forces [40]. In our formulation, nanoparticle irreversible aggregation is probably prevented by excipients for the majority of nanoparticles. However, some may stick together during the drying process, therefore explaining the size increase as well as the increase of the width of the distribution.

Table 1
Microparticle size distribution as a function of nanoparticle concentration

Nanoparticle concentration (%, w/w)	D_{10} (μm)	D_{50} (μm)	D_{90} (μm)	D[4.3] (μm)
0	1.1±0.1	6.7±0.1	16.8±0.1	8.0±0.1
9	1.2±0.1	6.8±0.1	16.1±0.6	7.9±0.2
23	1.0±0.1	6.3±0.4	15.6±1.9	7.5±0.5
33	1.1±0.1	6.4±0.4	15.2±0.7	7.4±0.4

($n=3$).
Data are expressed in terms of the particle diameter at 10%, 50% and 90% of the volume distribution (D_{10}, D_{50} and D_{90} respectively) and as the volume weighed mean particle size (D[4.3]).

3.4. Drug release from Trojan particles

The percentage of DXA released was calculated on the basis of the real content of DXA in the Trojan particles. We found a drug loading of 92±2% in the Trojan particles as compared with the amount found in nanoparticles before spray drying ($n=4$). This indicates that most of the loaded drug is preserved throughout the spray drying process. Fig. 4 presents dexamethasone release from Trojan particles under sink conditions. After 72 h, dexamethasone release profile exhibits a biphasic behaviour, which consists in a burst release of about 50% within the first hours, followed by a slower steady release phase with an additional release of 20% after 72 h. By contrast, free nanoparticles release about 90% of the loaded drug within the first 4 h. The initial burst which is faster for Trojan particles than for free nanoparticles, is most probably due to nanoparticle contact with ethanol during the spray drying process. Some drug is released during the mixing process with the ethanol/water mixture containing the excipients. This drug fraction is therefore not encapsulated within nanoparticles anymore and is readily available for release as soon as Trojan particles are hydrated. The rapidity of the burst effect for Trojan particles is very similar to results obtained with DPPC-HA microparticles encapsulating free dexamethasone (Gómez Gaete 2007, *submitted*). It further confirms the existence of a free fraction of the drug due to the contact with ethanol. Following the burst release, the DPPC-HA matrix probably prevents or slows down the release of dexamethasone from embedded nanoparticles, leading to the second part of the release profile.

Our release results are in agreement with some results from Hadinoto et al. [41] who reported that drugs are released more slowly from hybrid particles formulated with lipids than from 220 nm nanoparticles. Nevertheless, these authors report an opposite effect with nanoparticles smaller than 120 nm. They postulate that this is due to the exposition of nanoparticles to a

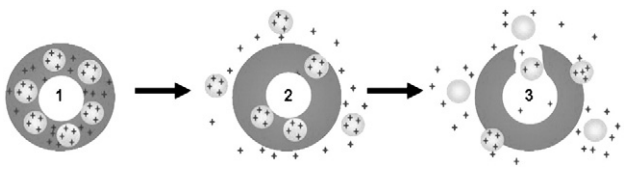

Fig. 7. Schematic of the different steps of DXA release from Trojan particles. After hydration (1), the free fraction of DXA associated to the DPPC-HA matrix is quickly released as well as loaded nanoparticles (2). These free nanoparticles then release DXA (3). Afterwards, the DPPC-HA matrix slowly release DXA loaded nanoparticles that once liberated release DXA, therefore explaining the observed slow release after the burst effect.

high temperature, which exceeds the glass transition temperature (T_g) of the polymer. In our case, DSC (DSC7, Perkin-Elmer, USA) analysis reveals that the T_g of the PLGA 75:25 nanoparticles is around 50 °C (not shown). Since the outlet temperature is approximately 54 °C, close to PLGA T_g, and since droplets spend a very short time at high temperature [42], it is very unlikely that the heat would modify drug dispersion within nanoparticles.

To conclude, one can finally postulate that DXA release from Trojan particles probably occurs in three different steps depicted in Fig. 7. After hydration, the free fraction of DXA associated to the DPPC-HA matrix is quickly released as well as loaded nanoparticles. These free nanoparticles then release DXA. Afterwards, the DPPC-HA matrix slowly release DXA loaded nanoparticles that once liberated release DXA, therefore explaining the observed slow release after the burst effect.

4. Conclusion

DXA encapsulation within PLGA nanoparticles was optimized for ocular delivery. The presence of crystalline drug along with the nanoparticles considerably reduces the ability to load the polymeric matrix. However, 1.3 mg DXM (=1.44 mg DXA) could be encapsulated into 100 mg nanoparticles, 6 fold more than what could be obtained using DXM. These nanoparticles have been easily formulated into Trojan particles using DPPC and HA as excipients. Neither Trojan particle density nor size distribution seem to be drastically modified as a function of nanoparticles concentration. *In vitro* release under sink conditions was performed for both nanoparticles and Trojan particles. Although a burst effect can be observed with both systems, the extent of the burst is lower for Trojan particles. The excipient matrix seems to provide protection to encapsulated nanoparticles and consequently to slow down drug release. Even if the active principle is released rather quickly as compared with other implants, the *in situ* release of drug loaded nanoparticles should favor their internalization within retinal pigment epithelial cells and might therefore increase the drug efficacy. This novel delivery system deserves to be evaluated *in vivo* to ascertain its interest for treating retinal affections.

Acknowledgements

C. Gómez-Gaete fellowship is supported by MECESUP Project UCO 0202 Ministerio de Educación, Chile and Universidad de Concepción, Chile. Authors acknowledge financial support from ANR, Jeunes Chercheurs (ANR05-JC42284) and would like to thank A. Allavena-Valette (CECM, Vitry ^{s}/Seine) for access to the SEM facility, V. Nicolas (IFR 141 ITFM, Châtenay-Malabry) for her help with confocal microscopy and M.P. Sánchez Olavarría (Universidad de Chile) for fruitful discussions.

References

[1] Y. Ogura, H. Kimura, Biodegradable polymer microspheres for targeted drug delivery to the retinal pigment epithelium, Surv. Ophthalmol. 39 (Suppl 1) (1995) S17–S24.

[2] A.L. Gomes dos Santos, A. Bochot, A. Doyle, N. Tsapis, J. Siepmann, F. Siepmann, J. Schmaler, M. Besnard, F. Behar-Cohen, E. Fattal, Sustained release of nanosized complexes of polyethylenimine and anti-TGF-beta 2 oligonucleotide improves the outcome of glaucoma surgery, J. Control. Release. 112 (3) (2006) 369–381.

[3] E. Fattal, C. Vauthier, in: J. Swarbrick, J.C. Boylan (Eds.), Encyclopedia of Pharmaceutical Technology, Marcel Dekker, Bâle, Suisse, 2002, pp. 1874–1892.

[4] P. Tewa-Tagne, G. Degobert, S. Briancon, C. Bordes, J.Y. Gauvrit, P. Lanteri, H. Fessi, Spray-drying nanocapsules in presence of colloidal silica as drying auxiliary agent: formulation and process variables optimization using experimental designs, Pharm. Res. 24 (4) (2007) 650–661.

[5] N. Tsapis, D. Bennett, B. Jackson, D.A. Weitz, D.A. Edwards, Trojan particles: large porous carriers of nanoparticles for drug delivery, Proc. Natl. Acad. Sci. U. S. A. 99 (19) (2002) 12001–12005.

[6] P. Tewa-Tagne, S. Briancon, H. Fessi, Spray-dried microparticles containing polymeric nanocapsules: formulation aspects, liquid phase interactions and particles characteristics, Int. J. Pharm. 325 (1–2) (2006) 63–74.

[7] S. Young, G. Larkin, M. Branley, S. Lightman, Safety and efficacy of intravitreal triamcinolone for cystoid macular oedema in uveitis, Clin. Experiment. Ophthalmol. 29 (1) (2001) 2–6.

[8] H. Tamura, K. Miyamoto, J. Kiryu, S. Miyahara, H. Katsuta, F. Hirose, K. Musashi, N. Yoshimura, Intravitreal injection of corticosteroid attenuates leukostasis and vascular leakage in experimental diabetic retina, Invest. Ophthalmol. Vis. Sci. 46 (4) (2005) 1440–1444.

[9] S. Munoz-Fernandez, E. Martin-Mola, Uveitis, Best. Pract. Res. Clin. Rheumatol. 20 (3) (2006) 487–505.

[10] R. Machemer, G. Sugita, Y. Tano, Treatment of intraocular proliferations with intravitreal steroids, Trans. Am. Ophthalmol. Soc. 77 (1979) 171–180.

[11] T. Ishibashi, K. Miki, N. Sorgente, R. Patterson, S.J. Ryan, Effects of intravitreal administration of steroids on experimental subretinal neovascularization in the subhuman primate, Arch. Ophthalmol. 103 (5) (1985) 708–711.

[12] G. Velez, S.M. Whitcup, New developments in sustained release drug delivery for the treatment of intraocular disease, Br. J. Ophthalmol. 83 (11) (1999) 1225–1229.

[13] D.P. Hainsworth, P.A. Pearson, J.D. Conklin, P. Ashton, Sustained release intravitreal dexamethasone, J. Ocul. Pharmacol. Ther. 12 (1) (1996) 57–63.

[14] G.J. Jaffe, D. Martin, D. Callanan, P.A. Pearson, B. Levy, T. Comstock, Fluocinolone acetonide implant (Retisert) for noninfectious posterior uveitis: thirty-four-week results of a multicenter randomized clinical study, Ophthalmology 113 (6) (2006) 1020–1027.

[15] G.J. Jaffe, P.A. Pearson, P. Ashton, Dexamethasone sustained drug delivery implant for the treatment of severe uveitis, Retina 20 (4) (2000) 402–403.

[16] C. Martinez-Sancho, R. Herrero-Vanrell, S. Negro, Poly (D,L-lactide-co-glycolide) microspheres for long-term intravitreal delivery of aciclovir: influence of fatty and non-fatty additives, J. Microencapsul. 20 (6) (2003) 799–810.

[17] F. Pavanetto, I. Genta, P. Giunchedi, B. Conti, U. Conte, Spray-dried albumin microspheres for the intra-articular delivery of dexamethasone, J. Microencapsul. 11 (4) (1994) 445–454.

[18] J. Filipovic-Grcic, D. Voinovich, M. Moneghini, M. Becirevic-Lacan, L. Magarotto, I. Jalsenjak, Chitosan microspheres with hydrocortisone and hydrocortisone-hydroxypropyl-beta-cyclodextrin inclusion complex, Eur. J. Pharm. Sci. 9 (4) (2000) 373–379.

[19] Y.C. Huang, C.H. Chiang, M.K. Yeh, Optimizing formulation factors in preparing chitosan microparticles by spray-drying method, J. Microencapsul. 20 (2) (2003) 247–260.

[20] P. Giunchedi, H.O. Alpar, U. Conte, PDLLA microspheres containing steroids: spray-drying, o/w and w/o/w emulsifications as preparation methods, J. Microencapsul. 15 (2) (1998) 185–195.

[21] E. Esposito, R. Roncarati, R. Cortesi, F. Cervellati, C. Nastruzzi, Production of Eudragit microparticles by spray-drying technique: influence of experimental parameters on morphological and dimensional characteristics, Pharm. Dev. Technol. 5 (2) (2000) 267–278.

[22] C.S. Chaw, Y.Y. Yang, I.J. Lim, T.T. Phan, Water-soluble betamethasone-loaded poly(lactide-co-glycolide) hollow microparticles as a sustained release dosage form, J. Microencapsul. 20 (3) (2003) 349–359.
[23] T. Sebti, K. Amighi, Preparation and *in vitro* evaluation of lipidic carriers and fillers for inhalation, Eur. J. Pharm. Biopharm. 63 (1) (2006) 51–58.
[24] G. Colombo, R. Padera, R. Langer, D.S. Kohane, Prolonged duration local anesthesia with lipid-protein-sugar particles containing bupivacaine and dexamethasone, J. Biomed. Mater. Res. A. 75 (2) (2005) 458–464.
[25] M.A. Ionita, R.M. Ion, B. Carstocea, Photochemical and photodynamic properties of vitamin B2-riboflavin and liposomes, Oftalmologia 58 (3) (2003) 29–34.
[26] N.N. Sanders, L. Peeters, I. Lentacker, J. Demeester, S.C. De Smedt, Wanted and unwanted properties of surface PEGylated nucleic acid nanoparticles in ocular gene transfer, Journal. of. Controlled. Release. 122 (3) (2007) 226–235.
[27] L. Lajavardi, A. Bochot, S. Camelo, B. Goldenberg, M.C. Naud, F. Behar-Cohen, E. Fattal, Y. de Kozak, Downregulation of endotoxin-induced uveitis by intravitreal injection of vasoactive intestinal peptide encapsulated in liposomes, Invest. Ophthalmol. Vis. Sci. 48 (7) (2007) 3230–3238.
[28] E.A. Balazs, in: D. Miller, R. Stegmann (Eds.), Healon (Sodium Hyaluronate): A Guide to its Use in Ophthalmic Surgery, John Wiley & Sons, New York, 1983.
[29] S.K. Hahn, S.J. Kim, M.J. Kim, D.H. Kim, Characterization and in vivo study of sustained-release formulation of human growth hormone using sodium hyaluronate, Pharm. Res. 21 (8) (2004) 1374–1381.
[30] E.A. Balazs, J.L. Denlinger, Viscosupplementation: a new concept in the treatment of osteoarthritis, J. Rheumatol. Suppl. 39 (1993) 3–9.
[31] K. Surendrakumar, G.P. Martyn, E.C. Hodgers, M. Jansen, J.A. Blair, Sustained release of insulin from sodium hyaluronate based dry powder formulations after pulmonary delivery to beagle dogs, J. Control. Release. 91 (3) (2003) 385–394.
[32] S.J. Kim, S.K. Hahn, M.J. Kim, D.H. Kim, Y.P. Lee, Development of a novel sustained release formulation of recombinant human growth hormone using sodium hyaluronate microparticles, J. Control. Release. 104 (2) (2005) 323–335.
[33] W. Lund, The Pharmaceutical CODEX, Principes and Practice of Pharmaceutics, The Pharmaceutical Press, London, 1994, p. 826.
[34] A.M. Layre, R. Gref, J. Richard, D. Requier, H. Chacun, M. Appel, A.J. Domb, P. Couvreur, Nanoencapsulation of a crystalline drug, Int. J. Pharm. 298 (2) (2005) 323–327.
[35] C. Gomez-Gaete, N. Tsapis, M. Besnard, A. Bochot, E. Fattal, Encapsulation of dexamethasone into biodegradable polymeric nanoparticles, Int. J. Pharm. 331 (2) (2007) 153–159.
[36] R. Vanbever, J.D. Mintzes, J. Wang, J. Nice, D. Chen, R. Batycky, R. Langer, D.A. Edwards, Formulation and physical characterization of large porous particles for inhalation, Pharm. Res. 16 (11) (1999) 1735–1742.
[37] J.O. Sham, Y. Zhang, W.H. Finlay, W.H. Roa, R. Lobenberg, Formulation and characterization of spray-dried powders containing nanoparticles for aerosol delivery to the lung, Int. J. Pharm. 269 (2) (2004) 457–467.
[38] K. Hadinoto, P. Phanapavudhikul, Z. Kewu, R.B. Tan, Dry powder aerosol delivery of large hollow nanoparticulate aggregates as prospective carriers of nanoparticulate drugs: effects of phospholipids, Int. J. Pharm. 333 (1–2) (2007) 187–198.
[39] K. Hadinoto, P. Phanapavudhikul, K. Zhu, R.B. Tan, Novel formulation of large hollow nanoparticles aggregates as potential carriers in inhaled delivery of nanoparticulate drugs, Ind. Eng. Chem. Res. 45 (10) (2006) 3697–3706.
[40] N. Tsapis, E.R. Dufresne, S.S. Sinha, C.S. Riera, J.W. Hutchinson, L. Mahadevan, D.A. Weitz, Onset of buckling in drying droplets of colloidal suspensions, Phys. Rev. Lett. 94 (1) (2005) 018302.
[41] K. Hadinoto, K. Zhu, R.B. Tan, Drug release study of large hollow nanoparticulate aggregates carrier particles for pulmonary delivery, Int. J. Pharm. 341 (1–2) (2007) 195–206.
[42] K. Masters, Spray Drying Handbook, Wiley, New York, 1991.